

¹²V. E. Naish, *Izv. Akad. Nauk SSSR Ser. Fiz.* 27, 1496 (1963) [*Bull. Acad. Sci. USSR Phys. Ser.* 27, 1468 (1963)].
¹³W. F. Brinkman and R. J. Elliott, *Proc. R. Soc. A* 294, 343 (1966).

¹⁴V. A. Koptsik and I. N. Kotsev, *JINR Preprint R4-8466*, Dubna, 1974.

Translated by W. F. Brown, Jr.

Magneto-resonance investigations of antiferromagnetic FeCl₃

F. V. Bragin, P. V. Vodolazskii, and S. M. Ryabchenko

Physics Institute, Ukrainian Academy of Sciences
 (Submitted November 18, 1975)
Zh. Eksp. Teor. Fiz. 70, 1539-1549 (April 1976)

The temperature dependence of the line width is investigated for ESR at $T > T_N$, for NMR of the Fe⁵⁷, Cl³⁵ and Cl³⁷ nuclei at $T < T_N$ and for AFMR in magnetically ordered FeCl₃. The critical exponent that describes the broadening of the ESR line as the temperature approaches $T_N = 9^\circ\text{K}$ is found to vary between 2.5 for $T > 22^\circ\text{K}$ and 0.56 for $T < 20^\circ\text{K}$. The NMR spectrum of Fe⁵⁷ corresponds to $H_{\text{hf}}(T \rightarrow 0) = 487$ kOe whereas the NMR spectrum of the Cl³⁵ and Cl³⁷ nuclei is almost continuous in the 20-55 MHz frequency range. The temperature dependence of the NMR spectrum is not described by a Brillouin function. The AFMR spectrum was observed in the 28 to 57 GHz frequency range. The frequency and field dependences of the AFMR spectral lines do not agree with those expected for a uniaxial antiferromagnet. A discussion of the results shows that they are consistent with the complex helicoidal magnetic structure of FeCl₃ obtained by neutron-diffraction measurements.

PACS numbers: 76.50.+g, 76.60.-k, 75.50.Ee

FeCl₃ crystals belong to the BiI₃ structure type (space group $R\bar{3}$)^[1] and are similar in structure to the layered ferromagnet CrBr₃. There are indications that FeCl₃ can go over at $T < 250^\circ\text{K}$ into a different structural form,^[2] but it is stated in^[3], where the magnetic structure was investigated by neutron diffraction, that the crystal structure of FeCl₃ in the magnetically-ordered state corresponds to that described in^[1] (Fig. 1) with slightly modified lattice parameters. An investigation of the susceptibility^[4] and of the Mössbauer effect^[5] have yielded the antiferromagnetic ordering temperature $T_N = 9.1^\circ\text{K}$, whereas a value $T_N = 15^\circ\text{K}$ is reported in^[3,6].

It is reported in^[3] that the magnetic structure of FeCl₃ is complicated and such that the spins of the Fe³⁺ ions that are closest to one another along the hexagonal axis are oppositely directed and lie in the crystallographic plane (1450) (hexagonal Miller indices), but the directions of the spins in the nearest adjacent planes of the (1450) type are rotated relative to one another through an angle $2\pi/15$. Thus, the antiferromagnetism vector forms a helical structure with a helix axis along the $[14\bar{5}0]$ directions and with a period equal to $15d$, where d is the distance between the nearest planes of the (1450) type. Measurements of the Mössbauer effect on Fe⁵⁷^[7] yield a value $H_{\text{hf}} = 487 \pm 15$ kOe for the hyperfine field. The measurements of the temperature dependence of H_{hf} in these studies are not accurate enough, and measurements in external magnetic fields^[5] do not allow us to state whether a helical magnetic structure is present or not, owing to the small values of the employed fields.

Taking into account the contradictory character of

the information on the magnetic properties of the FeCl₃ crystals, and also the interest in the helicoidal magnetic structures, we have carried out a group of investigations of FeCl₃ crystals, including the following: a) electron spin resonance (ESR) at $T > T_N$, b) nuclear magnetic resonance (NMR) in the magnetically ordered state, and c) antiferromagnetic resonance (AFMR).

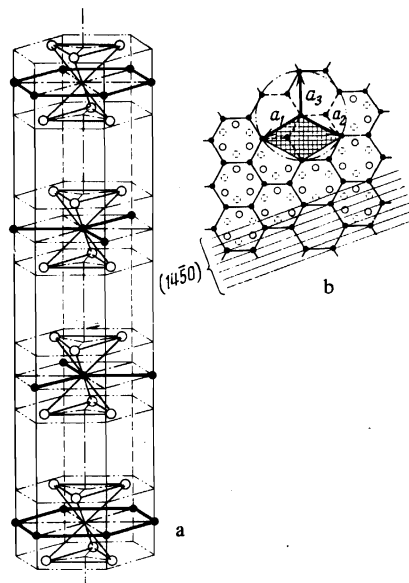


FIG. 1. a) $R\bar{3}$ crystal structure of FeCl₃; b) projection of the FeCl₃ "sandwich" on the (0001) plane: ●—Fe in the (00001) plane, ○—Cl above the (0001) plane, dashed circle—Cl below the (0001) plane. Shaded part—area of unit cell. a_1, a_2, a_3 axes of the chosen coordinate system. Straight lines—traces of the intersection of the (0001) plane with planes of the (1450) type.

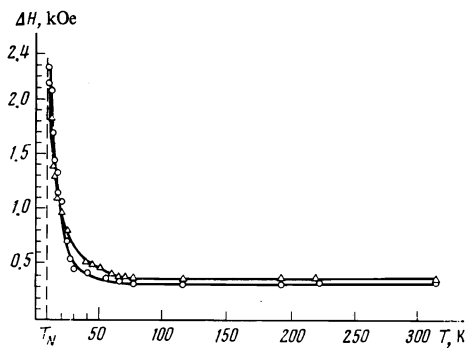


FIG. 2. Temperature dependence of the width of the ESR line: Δ — $C_3 \perp H_0$, \circ — $C_3 \parallel H_0$.

SAMPLES AND MEASUREMENT METHODS

Anhydrous FeCl_3 was synthesized by roasting chemically pure iron in a chlorine stream at $220 < T < 300^\circ\text{C}$. The obtained product was additionally purified by distillation in a Cl current at $T \sim 300^\circ\text{C}$, and was sealed in a quartz cell after forevacuum pumping and heating. The cell was placed in a furnace with temperature 306°C in the melting zone, and was slowly dropped (2 mm/h) to a region with large temperature gradient, after which the grown crystal was annealed. The obtained material was a concretion of large (up to $1.5\text{--}2\text{ cm}^3$) single-crystal blocks, which could be readily separated from one another. It should be noted that FeCl_3 is exceedingly hygroscopic, so that the preparation of the samples for the measurements and the storage of the grown crystals call for particular precautions. The crystals had a clearly pronounced basal plane, a property used to orient the samples. For NMR investigations we used single crystals measuring $5 \times 8 \times 25\text{ mm}$ and polycrystalline samples in hermetically sealed test tubes filled with dried CaCl_2 to protect against moisture. For the ESR and AFMR measurements we used single crystals measuring $0.5 \times 1.5 \times 3\text{ mm}$, sealed in paraffin or placed in fused lavsan-polyester envelopes.

The ESR measurements were performed in the 3-cm band with a type RE-1301 spectrometer provided with a cryostat with temperature controls (temperature maintained accurate to $\pm 0.05^\circ\text{K}$) in the interval $4\text{--}300^\circ\text{K}$. The AFMR measurements were performed with a setup described in^[8], and the NMR measurements were made by the spin-echo method with an installation of the IS-3 type equipped with a controlled cryostat ($1.5 < T < 300^\circ\text{K}$, accuracy $\sim \pm 0.2^\circ\text{K}$ at $T > 4.2^\circ\text{K}$). A superconducting solenoid was used for the NMR magnetic-field measurements.

EXPERIMENTAL RESULTS AND DISCUSSION

A. ESR temperature dependence of line width

One of the methods of determining the temperature of the antiferromagnetic transition is to investigate the behavior of the ESR line near the critical temperature. For different crystal symmetries, the ESR line becomes weaker and vanishes at $T \rightarrow T_N$, while for other symmetries (in particular, for uniaxial crystals), the ESR

undergoes critical broadening as the Néel temperature is approached.^[9-11] In this case

$$\Delta H(T) = \Delta H_\infty \left(\frac{T - T_N}{T} \right)^{-\beta}, \quad (1)$$

where $\Delta H(T)$ is the ESR line width at the given temperature, ΔH_∞ is the spin-spin contribution to the ESR line width at $T \gg T_N$, and β is the critical exponent. A theoretical calculation of the critical exponent β was carried out by different workers and its measurements were performed on many objects, but no reliable agreement between theory and experiment was reached, this being apparently a reflection of the high sensitivity of β to the details of the character of the exchange interactions and of the anisotropy of the concrete crystals. Nonetheless, the determination of β makes it possible to draw certain qualitative conclusions on the singularities of the antiferromagnetic transition, and approximation of the experimental data by (1) makes it possible to determine T_N . The ESR of FeCl_3 at $T \gg T_N$ constitute a single line ($g_{\parallel} = 2.015 \pm 0.008$, $g_{\perp} = 2.035 \pm 0.008$), the width of which increases with decreasing temperature.

The temperature dependence of the ESR line width was measured at frequencies 9300 and 7400 MHz. The line widths at these frequencies were the same at the same temperatures.

The ESR line does not change position within the limits of the measurement accuracy, and its width increases with decreasing temperature. At $T = 9^\circ\text{K}$, the line vanishes, although in a number of samples a weak and extremely broad line was observed at $T < 9^\circ\text{K}$, and is obviously due to partial hydration of the samples. In the entire temperature interval $T > 9^\circ\text{K}$, the line retains a Lorentz shape. The dependence of ΔH_L on T is shown in Fig. 2, while Fig. 3 shows the same dependence in coordinates $\log \Delta H_L$ and $\log [(T - T_N)/T]^{-1}$, where the value $T_N = 9^\circ\text{K}$, which follows from Fig. 2, was used. It is seen that the $\Delta H_L(T)$ dependence has three characteristic sections: 1) high-temperature, $T > 70^\circ\text{K}$, 2) intermediate, $25^\circ\text{K} < T < 60^\circ\text{K}$, and 3) low-temperature, $T < 20^\circ\text{K}$. The critical exponent β in the

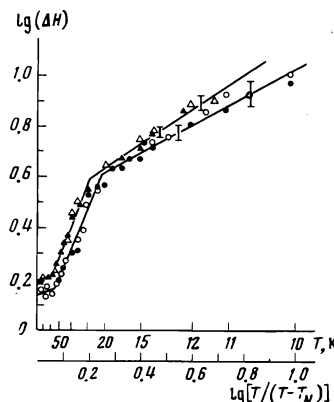


FIG. 3. Temperature dependence of the ESR line width in logarithmic coordinates: \circ —sample No. 1, $C_3 \perp H_0$; Δ —sample No. 1, $C_3 \parallel H_0$; \bullet —sample No. 2, $C_3 \perp H_0$; \blacktriangle —sample No. 2, $C_3 \parallel H_0$.

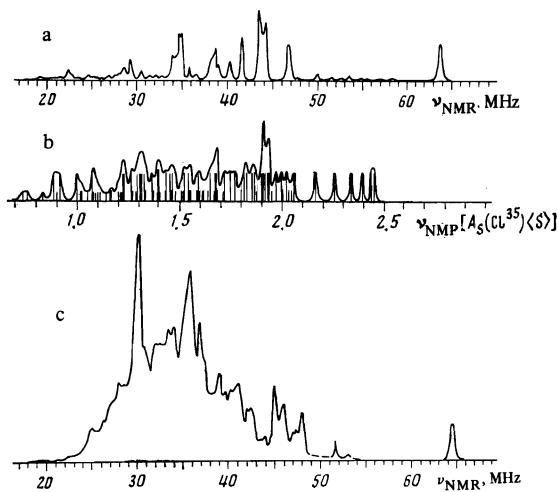


FIG. 4. NMR spectrum in FeCl_3 : a) $T = 4.2^\circ\text{K}$ ($H_{\text{ext}} = 0$); b) hypothetical NMR spectrum calculated for Cl^{35} (large strokes) and Cl^{37} (small strokes) ($H_{\text{ext}} = 0$); c) $T = 4.21^\circ\text{K}$ ($H_{\text{ext}} = 20$ kOe), $h_{\text{RF}} \parallel H \perp C_3$.

“low-temperature” section is equal to 0.56 ± 0.05 , which is close to the theoretical values obtained^[9, 12] for different models of the critical fluctuations, whereas in the “intermediate” section $\beta = 2.5$ is anomalously large, and finally, in the high-temperature section the dependence of the line width of the temperature is negligible. The values of ΔH_{ω} depend insignificantly on the crystal orientations relative to the external magnetic field, and are different in the three different temperature sections: $\Delta H_{\omega_{\parallel}} \approx \Delta H_{\omega_{\perp}} \approx 690 \pm 10$ Oe in the low-temperature section, $\Delta H_{\omega_{\parallel}} = 285$ Oe and $\Delta H_{\omega_{\perp}} = 263$ Oe in the intermediate section, and $\Delta H_{\omega_{\parallel}} = 367$ Oe and $\Delta H_{\omega_{\perp}} \times 324$ Oe in the high-temperature section. The anomalous value of β in the intermediate region, as well as the large width of this region, may indicate that in the intermediate region the short-range order fluctuations are connected with the relatively strong exchange interaction inside the layer, which, being “two-dimensional” because of the small anisotropy and the small value of the “three-dimensional” interaction between the layers, cannot lead to establishment of long-range magnetic order. At the same time, in the “low-temperature” region, there appear fluctuations of three-dimensional short-range order, due to the interaction between the layers, which leads to the usual value of β .

B. Nuclear magnetic resonance

The nuclear quadrupole resonance of the nuclei Cl^{35} in FeCl_3 was investigated by Narath.^[13] He observed at $T = 76^\circ\text{K}$ one broad line at a frequency 10.118 MHz. We were unable to observe by the spin-echo method any lines at $T > 7^\circ\text{K}$, possibly because of the short relaxation times T_1 and T_2 in the interval $T > 7^\circ\text{K}$. At $T < 7^\circ\text{K}$ we observe an NMR spectrum in the absence of an external magnetic field. The form of the spectrum at $T = 4.21^\circ\text{K}$ is shown in Fig. 4a. When an external magnetic field was applied in the basal plane of the single-crystal sample, perpendicular to the radio-frequency field h_{RF} , also located in the basal plane, the

spectral lines became weaker and were difficult to observe at fields > 10 kOe. Lines with frequencies lower than 60 MHz were furthermore regrouped in this case. Application of a magnetic field in the basal plane of the crystal parallel to the radio-frequency field caused some of the lines to shift from their positions, become weaker, and vanish, while the remaining lines were regrouped and became stronger. The line at 63.8 MHz shifted very little, changing only in intensity. The form of the spectrum in a 20-kOe field at $T = 4.2^\circ\text{K}$ is shown in Fig. 4c. The noted behavior of the spectrum in a magnetic field makes it possible to draw immediately definite conclusions. First, starting with weak fields, $H \gtrsim 1$ kOe, the directions of the spins become perpendicular to the static field H , which leads to an enhancement of the signal for $h_{\text{RF}} \parallel H$ and to a weakening at $h_{\text{RF}} \perp H$, inasmuch as the component h_{RF} perpendicular to the spin direction is responsible for the magnetic resonance. This points to antiferromagnetic ordering with small anisotropy, and the ordering is not of the “easy-axis” type. Second, it can be stated that the line at the frequency ~ 64 MHz and the remaining lines of the spectrum are of different origin. Comparison with the data on the Mössbauer effect shows that the ~ 64 MHz line is due to NMR of Fe^{57} [$H_{\text{hf}}(0) = 487$ kOe], whereas the remaining lines are due to NMR of Cl^{35} and Cl^{37} . Inasmuch as for Fe^{57} the main contribution to the hyperfine field H_{hf} is due to the interaction with its own electron shell, and H_{hf} is much larger than the employed external fields ($H \leq 20$ kOe), this line is not very sensitive to the external field. In addition, the smooth evolution of the spectrum of the Cl nuclei when a magnetic field is applied indicate that the turning of the spin takes place without a phase transition. The part of the spectrum which vanishes in the strong field is probably connected with antiferromagnetic domains resulting from the presence in the crystal of several equivalent ordering directions (planes).

Whereas the NMR spectrum of Fe^{57} is determined by interaction with its own electron shell, and only a single line exists when the spin of the Fe^{57} nucleus is equal to $1/2$ (the insignificant splitting of this line indicates the presence of a certain non-equivalence $\langle S \rangle$ for different ions in the lattice), the NMR of the Cl nuclei ($I = 3/2$) is determined by the interaction of at least two nearest Fe^{3+} ions. If we examine the structure of FeCl_3 (Fig. 1) from this point of view, then we obtain

$$\begin{aligned} \hat{\mathcal{H}}_{\text{hf}} = \langle S_i \rangle \left\{ I_x \left[(a_{\parallel} + a_{\perp}) \cos \varphi \sin \left(\theta + \frac{\delta_0}{2} \right) \cos \frac{\delta_0}{2} - (a_{\parallel} - a_{\perp}) \right. \right. \\ \times \left. \left. \left(\frac{1}{\sqrt{3}} \sin \varphi \cos \left(\theta + \frac{\delta_0}{2} \right) \sin \frac{\delta_0}{2} + \frac{2}{\sqrt{6}} \sin \left(\theta + \frac{\delta_0}{2} \right) \sin \frac{\delta_0}{2} \right) \right] \right. \\ \left. + I_y \left[\frac{1}{\sqrt{6}} (a_{\parallel} + 5a_{\perp}) \sin \varphi \sin \left(\theta + \frac{\delta_0}{2} \right) \cos \frac{\delta_0}{2} - (a_{\parallel} - a_{\perp}) \right. \right. \\ \times \left. \left. \left(\frac{1}{\sqrt{3}} \cos \varphi \cos \left(\theta + \frac{\delta_0}{2} \right) \sin \frac{\delta_0}{2} + \frac{2}{3\sqrt{2}} \cos \left(\theta + \frac{\delta_0}{2} \right) \cos \frac{\delta_0}{2} \right) \right] \right. \\ \left. + I_z \left[\frac{2}{3} (a_{\parallel} + 2a_{\perp}) \cos \left(\theta + \frac{\delta_0}{2} \right) \cos \frac{\delta_0}{2} + (a_{\parallel} - a_{\perp}) \right. \right. \\ \times \left. \left. \left(\frac{2}{\sqrt{6}} \cos \varphi \cos \left(\theta + \frac{\delta_0}{2} \right) \sin \frac{\delta_0}{2} - \sqrt{\frac{2}{3}} \sin \varphi \sin \left(\theta + \frac{\delta_0}{2} \right) \cos \frac{\delta_0}{2} \right) \right] \right\} + \hat{\mathcal{H}}_Q. \end{aligned} \quad (2)$$

Here $\langle S_i \rangle$ is the average value of the projection of the electron spin on its individual ordering direction (in a

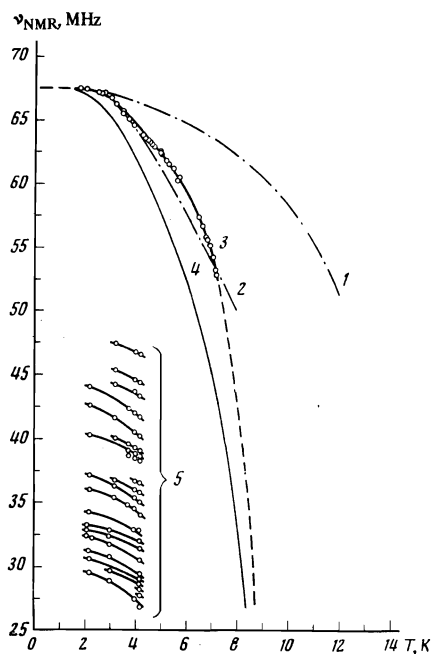


FIG. 5. Temperature dependence of the frequencies of the NMR transitions in FeCl_3 ($H_{\text{ext}} = 0$). Fe^{57} nuclei: 1—Mössbauer effect data^[7]; 2—neutron-diffraction data^[3]; 3—NMR experimental results; 4—Brillouin function $\sigma = B_S(3S\sigma/(S+1)\tau)$ for Fe ($S = 5/2$) at $T_N = 9^\circ\text{K}$. Cl^{35} and Cl^{37} nuclei: curve 5—experimental NMR results.

helicoidal structure, these directions will be different for the different spins, whereas $|\langle S_i \rangle|$ will be the same); the axes x , y , and z for the different Cl nuclei in the FeCl_3 structure are different—the x axis coincides with the direction of the Fe—Fe bond of the Fe^{3+} ions closest to the given Cl nucleus, the y axis is perpendicular to this direction, and the z axis is parallel to the axis of the crystal and is directed towards the investigated Cl nucleus (there are Cl^- ions above and below the plane containing the metal ions); a_{\parallel} and a_{\perp} are the constants of the hyperfine interaction of the Fe^{3+} ion with the Cl nucleus (the symbols \parallel and \perp pertain to the direction of the Fe—Cl bond); φ is the angle between the direction of the x axis and the plane containing the z axis, and the direction of the spins of the Fe ions: θ is the angle between the z axis and the spin direction of the first Fe^{3+} ion (the x axis is directed from the first Fe^{3+} ion to the second), while δ_0 is the angle between the direction of the spins of the first and second ions, and $\hat{\mathcal{H}}_Q$ is the Hamiltonian of the quadrupole interaction.

Analyzing (2) with account taken of the spectra of FeCl_3 , we find that in the case of collinear easy-plane ordering we should have three groups of nonequivalent Cl nuclei. Taking into account $I = 3/2$ and the presence of quadrupole moments of the chlorine nuclei, we should observe in a zero external field nine lines from each of the two isotopes Cl^{35} and Cl^{37} , but this does not agree with experiment. In the case of a helicoidal structure with helix axis $\{ikl0\}$, $9n$ lines should be observed from each isotope (n is the periodicity of the helicoid), i.e., for the structure obtained by Cable *et al.*^[3] there should be observed 135 lines from each isotope.

Naturally, such a spectrum should be practically continuous, and the intensity distribution in it will be determined by the line density per unit frequency interval, which depends on the relation between a_{\parallel} , a_{\perp} , and $e^2q_{zz}Q$. Recognizing that $(a_{\parallel} - a_{\perp})$, as a rule, is small in comparison with $A_S = (a_{\parallel} + 2a_{\perp})/3$, we have plotted a hypothetical summary NMR spectrum of both Cl isotopes under the assumption that $a_{\parallel} = a_{\perp}$, and neglecting the quadrupole splitting. In this case, the NMR spectrum for each Cl isotope in FeCl_3 is represented by $3n = 45$ lines. Their positions for Cl^{35} on a frequency scale in units of $A_S^{35}\langle S_i \rangle$ were calculated from (2) and are shown in Fig. 4b by large vertical strokes. The positions of the NMR spectral lines of the isotope Cl^{37} are shown on the same frequency scale (small strokes) with allowance for the fact that $A_S^{35}/A_S^{37} = \mu^{35}/\mu^{37} = 1.201$. The height of the strokes reflect the intensity of the NMR signals of the Cl^- isotopes in accordance with their natural abundance. The envelope of the spectrum was drawn under the assumption that the width of the line corresponding to each stroke, ~ 0.2 in $A_S^{35}\langle S \rangle$ units, and the intensity is proportional to the height of the stroke. A qualitative examination of the transformation of the "hypothetical" spectrum in a magnetic field under the assumption that H is parallel to the helix axis and that the spins become inclined to the field direction with increasing H without changing the pitch of the helix, shows that the spectrum should become compressed towards the center when the external field is applied. Naturally, the hypothetical spectrum cannot be compared in detail with the experimental, in view of the rough assumptions made, but such qualitative characteristics as the ratio of the maximal and minimal frequencies in the spectrum and the grouping of the lines in the central part of the spectrum allow us to state that the experimentally observed spectrum indicates that FeCl_3 has a many-sublattice or helical magnetic structure, and does not contradict the magnetic structure proposed in^[3]. It is also possible to estimate the values of $A_S\langle S_i \rangle$ in frequency units $A_S^{35}\langle S_i \rangle \approx 20$ MHz, which leads, in accordance with the arguments presented in^[14], to an electron density $\alpha_S \approx 0.96\%$ for the $3d$ electron of Fe^{3+} on the $3s$ orbit of Cl^- ; this is somewhat larger, albeit of the same order, than the value of the analogous parameter for NiCl_2 , CoCl_2 , and FeCl_2 .^[14] This result, which indicates that the degree of s -hybridization of the metal-halide bond in FeCl_3 is increased in comparison with NiCl_2 , CoCl_2 , FeCl_2 , agrees with the increase of the quadrupole interaction in this compound in comparison with di-halides.

The temperature dependence of the NMR spectrum in a zero external field is shown in Fig. 5. We have paid principal attention to the investigation of the signal from the Fe^{57} nuclei, since this signal is practically insensitive to the complicated magnetic structure and its frequency is proportional to $\langle S_i \rangle$, whereas the distribution of the intensities in the spectrum of the chlorine nuclei depends on additional factors. But nonetheless, the dependence of the NMR frequencies of the Cl and Fe^{57} nuclei is qualitatively of the same type. For comparison, the figure shows the data of the Mössbauer experiments^[7] and the Brillouin curve for $S = 5/2$

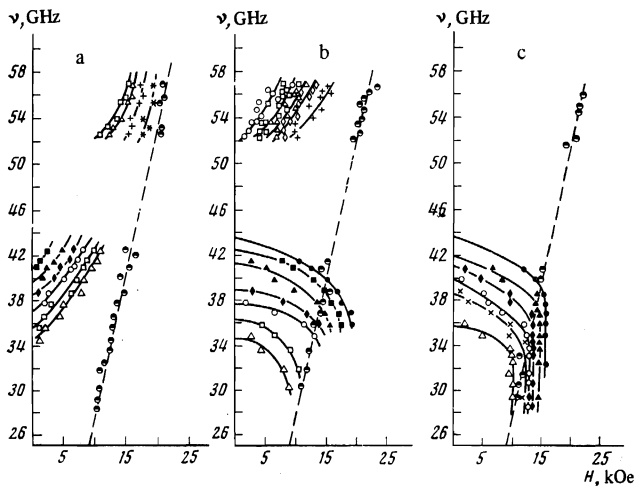


FIG. 6. Frequency-field dependences of AFMR in the temperature range 4.2–9.1°K: a) $C_3 \parallel H_0 \perp h_{micr}$; b) $(C_3 H_0) = 60^\circ$, $H_0 \perp h_{micr}$; c) $C_3 \perp H_0 \perp h_{micr}$. Symbols: ●—4.7 K, ■—4.9 K, ▲—5.21 K, ◆—5.48 K, ○—5.71 K, ×—5.85 K, □—6.05 K, △—6.35 K, +—6.85 K, *—7.46 K, ⊖—9.4 K, ◇—6.56 K.

at $T_N = 9^\circ\text{K}$. As seen from Fig. 5, $\nu_{NMR} \text{Fe}^{57}(T)$ has a gently sloping section at $T < 3^\circ\text{K}$, an almost linear section in the region $3^\circ\text{K} < T < 6^\circ\text{K}$, and a steep decrease at higher temperatures. The transverse relaxation time T_2 starting with $T_2 = 60 \mu\text{sec}$ at $T = 4.2^\circ\text{K}$ decreases with increasing temperature; on the $4.2\text{--}5.2^\circ\text{K}$ section it is linear with a rate $40 \mu\text{sec/deg}$; on the $5.2\text{--}7^\circ\text{K}$ section it varies like $26(T_N/N - 1)$ at $T_N = 9^\circ\text{K}$. At $T > 7^\circ\text{K}$, the spin-echo method becomes ineffective, and therefore the section with the steep decrease of the magnetization (Fig. 5) cannot be investigated in sufficient detail. The presence of a gently sloping section can be regarded as evidence of the presence, in the spin-wave spectrum of the crystal, of an energy gap with $\Delta E = k \times 3^\circ\text{K} \approx 2 \text{ cm}^{-1}$ (k is the Boltzmann constant), which should correspond to the AFMR frequencies on the order of 60 GHz in a zero field as $T \rightarrow 0$. The nearly linear decrease in the next temperature interval indicates that the magnetic interactions in the crystal are essentially two-dimensional.

The NMR spectrum of the Cl nuclei is not substantially transformed when the temperature is varied, thus indicating stability of the magnetic spectrum (invariance of the period of the helicoid).

C. Antiferromagnetic resonance

The AFMR spectrum was investigated in the frequency interval 26–42.5 and 52.5–57 GHz and in the temperature interval 4.2–9°K. Above 9°K, the observed ESR spectrum at the indicated frequencies is analogous to that described in Sec. A). At the experimental geometry $H_0 \parallel h_{micr} \perp C_3$ (C_3 is the crystal axis), no absorption was observed in the indicated frequency interval. We observed AFMR absorption at geometries $H_{micr} \perp H_0 \parallel C_3$, $h_{micr} \perp H_0 \perp C_3$, and $h_{micr} \perp H_0$, and with C_3 making a definite angle with H_0 . The measurements were made complicated by the fact that the dimensions of the sam-

ples were comparable with the length of the microwave, but this effect was filtered out by comparing the results obtained with samples having different geometric shapes. A characteristic feature of the absorbed lines is that they are observed only in weak fields, becoming weaker with increasing field. Therefore, in fields above 20 kOe (and also at frequencies below 28–29 GHz), we were unable to observe AFMR lines. The frequency-field dependences of the observed spectra at different temperatures are shown in Fig. 6. Figure 7 shows plots of AFMR at different temperatures for one of the frequencies. It should be noted that in practically all the cases, with the exception of the $\nu(H)$ lines, which are shown in Fig. 6, additional weaker lines were observed, the frequency-field dependences of which are difficult to trace because of the overlap with the strong lines. Qualitatively, however, it can be noted that for the experimental geometry of the type of Fig. 6a, the additional lines behaved in analogy with the principal lines in the geometry of Fig. 6c, and conversely, at the geometry of Fig. 6b, the number of additional lines was the largest. In the geometry of Fig. 6c, the principal and additional lines in the frequency interval 52–57 GHz were of comparable intensity, so that we were unable to separate the behavior of the individual lines, and these lines are not shown in Fig. 6c. In practically all the samples, simultaneously with the lines shown in Figs. 6a, 6b, and 6c, a broad ESR-like line was observed, with intensity comparable with that of the AFMR lines, but the ratio of its intensity to the intensities of the lines produced only in the antiferromagnetic state varied from sample to sample. This line may be a low-frequency ESR-like AFMR line, and the variation of its intensity is connected with the random character of the placements of the external and microwave magnetic fields relative to the directions in the basal plane of the crystal. Another cause of the onset of the ESR-like line is partial hydration of the samples or the presence of defects in them.

The observed AFMR spectra do not correspond to the spectra that can be expected in the case of a simple

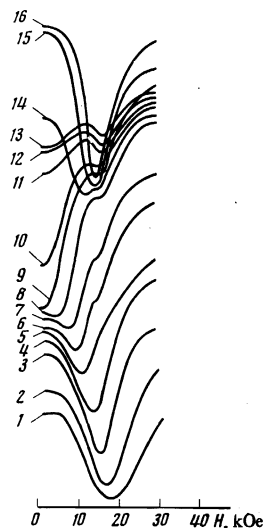


FIG. 7. Family of plots of AFMR spectra ($\nu = 40.28 \text{ GHz}$, $C_3 \perp H_0 \perp h_{micr}$) at different temperatures (in degrees K): 1—4.2; 2—4.38; 3—4.55; 4—4.7; 5—4.94; 6—5.1; 7—5.21; 8—5.48; 9—5.71; 10—5.85; 11—6.05; 12—6.35; 13—6.56; 14—6.85; 15—8.2; 16—9.1.

magnetic structure. They are closer in character to the possible spectra of a rhombic antiferromagnet, but the presence of additional lines and the variation of the line intensities with increasing magnetic field indicate that the spectrum contains more than two AFMR branches, and the microwave polarization necessary to observe the AFMR seems to depend on the field. Thus, properties of AFMR may correspond to a helicoidal structure, but a more detailed analysis of the experimental data can be based only on a theoretical investigation of the spin-wave spectrum of the proposed magnetic structure.

CONCLUSION

Thus, the presented aggregate of investigations points to a complex magnetic structure of FeCl_3 and does not contradict the antiferromagnetic helicoid structure.^[3] A definite part of the details of the experimental results lies outside the scope of the present article, but their discussion, as well as a more detailed analysis of the presented principal (from our point of view) results, call for a special theoretical consideration.

The authors are grateful to L. A. Kupriyanova, V. S.

Frolova, and A. A. Motuz for help with the crystal growth.

- ¹Crystal Structures 2, ed. R. W. G. Wyckoff, IS, New York, 1967; Gregory, J. Am. Chem. Soc. **73**, 472 (1951).
- ²D. E. Earles, R. C. Axtmann, V. Hazony, and I. Lefkowitz, J. Phys. Chem. Solids **29**, 1859 (1968).
- ³W. Cable, M. K. Wilkinson, E. O. Wollan, and W. G. Kocheler, Phys. Rev. **127**, 714 (1962).
- ⁴Edwin R. Jones, Jr., O. B. Morton, L. Cathey, Theo. Auel, and E. L. Amma, J. Chem. Phys. **50**, 4755 (1969).
- ⁵J. P. Stampel, W. T. Oosterhuis, and F. de S. Barros, J. Appl. Phys. **42**, 1721 (1971).
- ⁶M. K. Wilkinson, J. W. Cable, and E. O. Wollan, Bull. Am. Phys. Soc. **5**, 458 (1960).
- ⁷C. W. Kocher, Phys. Lett. **A24**, 93 (1967).
- ⁸A. F. Lozenko and S. M. Ryabchenko, Pis'ma Zh. Eksp. Teor. Fiz. **16**, 332 (1972) [JETP Lett. **16**, 234 (1972)].
- ⁹H. Mori and K. Kawasaki, Prog. Theor. Phys. **28**, 971 (1962).
- ¹⁰H. Mori, Prog. Theor. Phys. **30**, 576, 578 (1963).
- ¹¹S. Maekawa, J. Phys. Soc. Jap. **33**, 573 (1972).
- ¹²D. L. Huber, Phys. Rev. **B6**, 3180 (1972).
- ¹³A. Narath, J. Chem. Phys. **40**, 1169 (1964).
- ¹⁴F. V. Bragin and S. M. Ryabchenko, Fiz. Tverd. Tela **15**, 1050 (1973) [Sov. Phys. Solid State **15**, 721 (1973)].

Translated by J. G. Adashko

Parametric generation of phonons

S. A. Bulgadaev, B. I. Kaplan, and I. B. Levinson

L. D. Landau Institute of Theoretical Physics, USSR Academy of Sciences
(Submitted November 20, 1975)
Zh. Eksp. Teor. Fiz. **70**, 1550-1565 (April 1976)

A theory of parametric generation of short-wave acoustic phonons during the two-phonon absorption of infrared radiation is constructed. The generation thresholds and the nature of the prethreshold nonequilibrium-phonon distribution arising in broad- and narrow-band pumping are found. As a mechanism limiting the growth of the number of phonons near the threshold, the merging of nonequilibrium phonons into phonons of a higher equilibrium branch is considered. Such a mechanism turns out to be effective only for broad-band pumping. The results of the paper can easily be extended to the case when the phonon generation is effected by the beats of two light beams in the optical range.

PACS numbers: 78.20.Hp

INTRODUCTION

Orbach^[1] first drew attention to the fact the decay of a long-wave optical phonon into two short-wave acoustic phonons ($O \rightarrow 2A$) is a parametric process, and that, therefore, in generating optical phonons with the aid of light ($\nu - O$), we can expect the appearance of an instability in the system of acoustic phonons. The instability threshold should be especially low for decay into transverse acoustic phonons (TA), whose lifetime is anomalously long.^[2]

The corresponding experiment was performed by Colles and Giordmaine.^[3] The indubitable result of the experiment is the generation of nonequilibrium acoustic phonons, but the existence of a sharply defined threshold does not follow from it.

The theory developed in^[4] showed that there is no parametric instability in the process $\nu - O - 2A$. The point is that as the light intensity and, hence, the acoustic-phonon concentration increase, the rate of decay of the optical phonons also increases, since their decay becomes stimulated. As a result, the growth of the optical-phonon concentration slows down, and it turns out that this concentration reaches saturation, not having attained the threshold value. The same result was obtained by Sparks and Chow.^[5]

As can be seen from these arguments, the absence of the acoustic-phonon instability is due to the presence of a real intermediate particle (the optical phonon). Such a situation obtains only in resonance pumping, when the light frequency ν_0 is close to the optical-pho-